Check for updates

Supersolubility and solubility of lithium phosphate in sodium carbonate solution†

Huaiyou Wang, [ID] [ac] Jia Zhang,[ac] Xu Liu,[ac] Haiwen Ge,[ac] Zhibo Luo*[ab] and Min Wang [ID] *[ac]

The tail liquid generated from lithium carbonate production in salt lake brine is termed lithium-bearing mother liquor. This mother liquor exhibits a complex composition, with the Li^+ concentration typically around 1.5 g L^{-1}, representing a significant lithium resource. Preparing lithium phosphate (Li_3PO_4) from this mother liquor is critical for efficient lithium recovery. However, the lack of data on the thermodynamic behavior and Li_3PO_4 crystallization in such complex solutions has hindered the high-efficiency recovery of lithium resources. In this study, the solubility of Li_3O_4 in sodium carbonate solutions was determined using the dynamic dissolution equilibrium method. The effects of temperature and sodium carbonate concentration on solubility were analyzed, and experimental data were correlated using an exponential equation. Results indicated that the solubility of Li_3PO_4 in pure water and sodium carbonate solutions increases with temperature and sodium carbonate concentration. The supersolubility of Li_3PO_4 in $LiCl–Na_2CO_3$ electrolyte solutions was measured *via* turbidimetric analysis, and the metastable zone width (MSZW) was determined. The supersolubility of Li_3PO_4 significantly decreased with rising temperature. In contrast, supersolubility initially increased and then decreased with higher Na_2CO_3 concentrations, with reactant concentration being the decisive factor driving the crystallization reaction. Furthermore, the MSZW narrowed at elevated temperatures. Thermodynamic functions (ΔS_d, ΔH_d, and ΔG_d) for the dissolution process were calculated *via* the van't Hoff equation, confirming that Li_3PO_4 dissolution is a spontaneous and endothermic process. Based on solubility and supersolubility data, a novel process was developed to prepare battery-grade Li_3PO_4 (purity: 99.80%) from salt lake mother liquor. The results of Raman, FTIR, TG and SEM suggested that the prepared lithium phosphate was pure phase. This study provides fundamental physicochemical data and theoretical insights for the efficient separation and extraction of lithium resources from lithium precipitation mother liquor.

1. Introduction

The rapid growth of new global energy industries has underscored the importance of developing and utilizing lithium resources, which play a pivotal role in renewable energy applications.[1,2] As the world transitions towards carbon neutrality, lithium has emerged as a crucial raw material for lithium-ion batteries, making it indispensable for electric vehicles, energy storage systems, and various electronic devices, resulting in a significant increase in market demand.[3–5] Consequently, ensuring the efficient development and utilization of lithium resources and maintaining a stable supply chain have become

a shared objective among researchers. Current methods for lithium extraction primarily include the recovery of lithium from salt lake brines and mineral ores.[6–8] Salt lake brine extraction techniques typically involve processes such as solvent extraction,[9,10] ion exchange,[11,12] precipitation,[13,14] and membrane separation[15–17] to concentrate and separate lithium ions, ultimately yielding lithium compounds. China possesses abundant lithium resources in its salt lakes, with their reserves accounting for 83% of the nation's total lithium resources.[18] However, challenges such as harsh environmental conditions, varying brine grades, and high Mg/Li ratios complicate the extraction process.[7,19] Addressing these challenges and advancing extraction technology are crucial for the efficient utilization of salt lake resources and for supporting the development of the new energy sector. The mainstream processes for lithium extraction from salt lakes with high magnesium-to-lithium ratios primarily include the following steps: magnesium–lithium separation, impurity removal from lithium-bearing solutions, and lithium carbonate precipitation/

[a]Key Laboratory of Green and High-end Utilization of Salt Lake Resources, Qinghai Institute of Salt Lakes, Chinese Academy of Sciences, Xining, 810008, PR China

[b]Minmetals Salt Lake Co., Ltd, Xining, 810000, PR China

[c]Qinghai Provincial Key Laboratory of Resources and Chemistry of Salt Lakes, Xining, 810008, PR China

† Electronic supplementary information (ESI) available. See DOI: https://doi.org/10.1039/d5ra02716k

conversion. Among these, the lithium carbonate precipitation step involves adding sodium carbonate solution to a lithium-enriched solution to produce lithium carbonate (Li_2CO_3) *via* precipitation. Solid–liquid separation subsequently generates a lithium carbonate mother liquor, also referred to as brine lithium extraction mother liquor. This alkaline mother liquor retains a lithium concentration of 1.0 to 2.5 g L^{-1} and contains major components such as Na^+, Li^+, Cl^-, and CO_3^{2-}. As a critical resource, lithium urgently requires efficient recovery and utilization.[20–23]

Li_3PO_4, a high value-added lithium compound, has gained attention due to its applications in lithium-ion batteries,[24,25] catalysts,[26,27] and other advanced materials.[28,29] With its low solubility ($K_{sp} = 2.37 \times 10^{-11}$ at 25 °C), Li_3PO_4 can precipitate efficiently from solutions even at low lithium concentrations, making it a promising candidate for enhancing lithium recovery rates.[30,31] Liu Dongfu *et al.*[32] prepared an anolyte solution by electrochemically deintercalating lithium from salt lake brine with a high Mg/Li ratio, using phosphate precipitation to remove impurities. By optimizing factors such as the initial lithium concentration, precipitation time, precipitant dosage, and reaction temperature, combined with anhydrous ethanol and seed crystal induction, a lithium precipitation rate of 82.5% was achieved, yielding a relatively pure Li_3PO_4 product. Sun Jianzhi *et al.*[33] utilized tailings from salt lake lithium extraction to precipitate Li^+ as Li_2CO_3, which was then mixed with Na_3PO_4 solution, adjusted to pH 11, and reacted in a high-pressure reactor at 120–150 °C for 3 to 10 hours. The resulting Li_3PO_4 particles, with sizes of 5–8 μm, enabled a lithium yield of 90% to be achieved. Furthermore, Zhu Jun *et al.*[34] produced high-purity, uniform lithium phosphate powder by removing impurities from crude lithium phosphate using oxalate precipitation and a two-stage ion exchange process. These studies provide a solid foundation for enhancing lithium resource utilization efficiency to meet diverse market needs.

Generally, in the crystallization process of Li_3PO_4, solubility, supersolubility, and metastable zone width (MZW) are core parameters requiring critical consideration. Industrial crystallization is typically controlled within the metastable zone to obtain products with high purity, high yield, ideal morphology, and uniform particle size distribution. Supersolubility and metastable zone width are often influenced by factors such as temperature, impurities, feeding rate, and solution kinetics. The mother liquor after Li_2CO_3 precipitation contains abundant carbonate ions, which may exert complex effects on Li_3PO_4 crystallization behavior. To our knowledge, no data on Li_3PO_4 solubility or supersolubility in the carbonate impurity system have been documented. Additionally, reported data on Li_3PO_4 solubility in aqueous solutions at the same temperature ranges have discrepancies, possibly due to the hydrolysis of phosphate ions. Specifically, the solubilities determined at 298.15 K were reported as 0.0270%,[35] 0.0297% and 0.0239%.[36] In this study, the influence of experimental parameters (*e.g.*, temperature and sodium carbonate concentration) on Li_3PO_4 solubility, supersolubility, and MZW was investigated. Based on the observed patterns of Li_3PO_4 solubility, supersolubility, and MZW

variations, a battery-grade Li_3PO_4 precipitate from the lithium-bearing mother liquor was obtained.

2. Experimental

2.1 Chemicals

The reagents used in this study included lithium phosphate (Li_3PO_4, 99.9%, McLean), sodium carbonate (Na_2CO_3, 99.9%, McLean), lithium chloride (LiCl) (99.9%, Macklin), sodium hydroxide (NaOH) (99.0%, Macklin), and concentrated hydrochloric acid (36–38%, Macklin). All chemicals were used as received without further purification. Deionized water (resistivity 18.25 MΩ cm) was prepared with an ultra-pure water preparation system (UPT-II-20T, Chengdu Ultra-Pure Technology Co., Ltd).

2.2 Solubility determination

The solubility of Li_3PO_4 in Na_2CO_3 solutions was determined using a static isothermal dissolution method. A series of Na_2CO_3 solutions with different mass fractions were prepared and transferred into polytetrafluoroethylene (PTFE) bottles. These bottles were placed in a thermostatic water bath with a temperature control accuracy of ±0.01 °C, and heated to the desired temperature. Subsequently, 1.5 g of solid Li_3PO_4 was added to each bottle and the solutions were stirred at a constant temperature until equilibrium was reached. Once equilibrium was achieved, the solid and liquid phases were separated and the lithium ion concentration in the liquid phase was measured using inductively coupled plasma optical emission spectrometry (ICP-OES). The measured lithium ion concentrations were then used to calculate the solubility of Li_3PO_4 in each solution. The solid phase was analyzed by XRD.

2.3 Supersolubility and solubility determination

Fig. 1(a) displays the CrystalSCANPolyBlock system (E1061, HEL LIMITED) used for measuring supersolubility. The crystallizer consisted of a 100 mL glass reactor with an internal overhead stirrer and temperature and turbidity sensors controlled by the PolyBlock. The turbidity sensor detected crystal nuclei with an IR laser reflected by an optical lens. The temperature was controlled with the PolyBlock through a thermostatic bath (FP-50, JULABO Labortechnik GmbH).

To measure supersolubility, 70.0 g (2 g L^{-1}) LiCl solution was settled in the crystallizer, and the overhead stirrer, temperature probe and turbidity probe were immersed in the solutions. The CrystalSCANPolyBlock system and thermostatic bath were then initiated with a stirring rate of 250 rpm and the solution temperature was kept constant. A Na_3PO_4 solution (wt 8%) was pumped into the LiCl solution, except when assessing the impact of Na_2CO_3 concentration on Li_3PO_4 supersolubility, *via* a liquid dosing system at a feeding rate of 1 mL min^{-1}. Upon nucleation, as indicated by a rapid rise in the turbidity curve, pumping of the solution was stopped and the time interval between the initial pumping and nucleation was recorded as the pumping time. Supersolubility was determined based on the added amount of Na_3PO_4, which was calculated based on
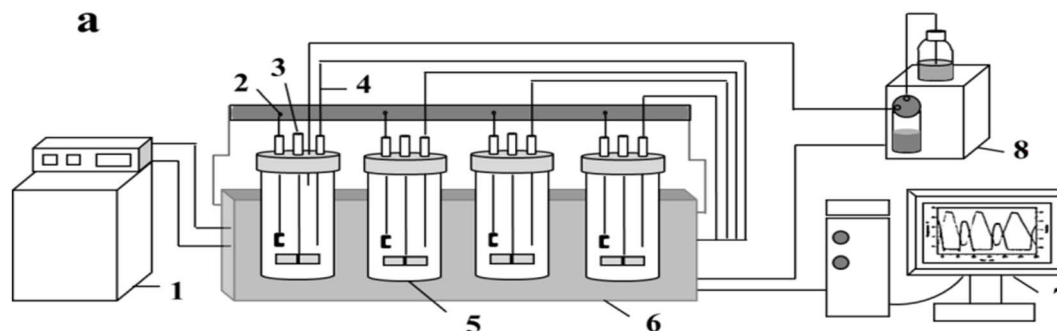
Fig. 1   1-Low-temperature thermostat tank; 2-turbidity probe; 3-suspension stirring paddle; 4-temperature probe; 5-crystallization reactor; 6-four-channel reaction platform; 7-control system; 8-liquid dosing system.

concentration, feeding rate, and pumping time. Each measurement was repeated twice to verify the experimental reproducibility. The supersolubility and solubility of Li_3PO_4 in electrolyte solutions are represented by c_{super} and c_{sol}, respectively. The difference between the supersolubility and solubility is defined as the MSZW ($\Delta c = c_{super} - c_{sol}$).

2.4   Preparation of battery-grade lithium phosphate

The process flow for the preparation of battery-grade Li_3PO_4 is shown in Fig. 1. The preparation process uses a fully automatic anti-solvent crystallization screening instrument as the synthesis equipment. The equipment allows for precise control of reaction conditions such as temperature, stirring speed, and feeding speed through program settings. The raw material was lithium-bearing mother liquor from a salt lake in the Qaidam Basin (composition shown in Table 1). First, concentrated hydrochloric acid was used to adjust the pH of the lithium precipitation mother liquor to 7.0 to remove some carbonate ions. Then, a 30% sodium hydroxide solution was added to adjust the pH to 13.0, followed by the dropwise addition of 8% sodium phosphate for the precipitation reaction. The crude product obtained was further processed using a hydrochloric acid recrystallization method to produce battery-grade Li_3PO_4.

FTIR spectroscopy analysis was conducted with a Nicolet Nexus 670 FTIR spectrophotometer (Thermo Nicolet Corporation, Madison, WI, USA) in solid films using KBr salt tablets in a range of 500–4000 cm^{-1}. Raman spectra were recorded at 25 °C with a Raman spectrometer (DXR, Thermo Fisher Scientific, USA).

The thermal stability of Li_3PO_4 was measured by TG-DSC (Mettler Toledo, TGA/DSC3+). The measurements were carried at a temperature range of 30–900 °C with a heating rate of 10 °C min^{-1}. The blowing gas was nitrogen with a blowing flow rate of 50 mL min^{-1}. A 100 μL platinum crucible with a perforated cover was used for measurement.

The morphology of Li_3PO_4 was examined by SEM (JSM-5610LV, JEOL, Japan) in combination with energy dispersive X-ray spectroscopy mapping (X-MAXN).

3.   Results and discussion

3.1   Solubility of lithium phosphate in Li_2CO_3 solution

Based on the data listed in Table S1,† when the dissolution equilibrium time was more than 48 h, the solubility of Li_3PO_4 remained stable. Thus, a 48-hour equilibrium time was adopted to determine the Li_3PO_4 solubility in this study.

Table 2 shows the solubility of Li_3PO_4 in aqueous solution ranging from 298.15 K to 353.15 K. It is noted that the solubility increased with increasing temperature. A solubility of 0.0244% at 298.15 K was consistent with the reported value,[36] but marginally higher than that reported[37] at higher temperature. This is because the reported values showed a fluctuating correlation with the rising temperature.

Using the solubility exponential model equation (eqn (1), the data across various temperatures were fitted as depicted in Fig. 2 with a correlation coefficient of $R^2 = 0.9837$. The relative errors between the calculated solubility values and the experimental data are presented in Table 3, with all errors within

Table 2   Solubility of Li_3PO_4 in aqueous solution at 293.15 K–353.15 K

T/K	Solubility of Li_3PO_4 (%)	Solid phase
298.15	0.0244	Li_3PO_4
303.15	0.0283	Li_3PO_4
313.15	0.0327	Li_3PO_4
323.15	0.0358	Li_3PO_4
333.15	0.0376	Li_3PO_4
343.15	0.0405	Li_3PO_4
353.15	0.0437	Li_3PO_4

Table 1   Lithium-bearing mother liquor composition (g L^{-1})

Sample	ρ (g cm^{-3})	Li^+	Mg^{2+}	Ca^{2+}	Na^+	Cl^-	CO_3^{2-}	OH^-	B_2O_3	SO_4^{2-}
Mother liquor	1.1685	1.36	0.002	0.003	49.39	60.46	17.33	2.35	0.44	0.17
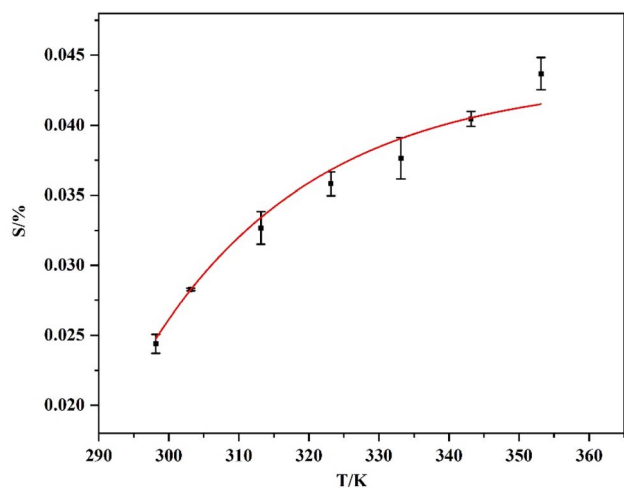
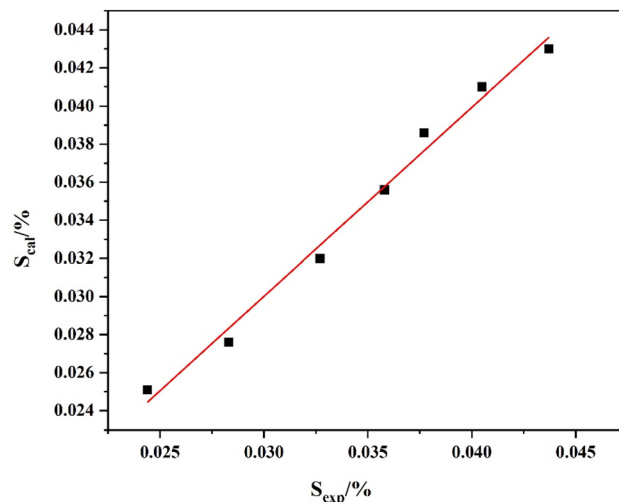Fig. 2 Exponential form of the solubility of lithium phosphate in water as a function of temperature.

Fig. 3 Correlation between the experimental and exponential calculated values of lithium phosphate solubility in water at different temperatures.

Table 3 Experimental values for the solubility of lithium phosphate in water, calculated values in exponential form and relative errors

Temperature/K	Experimental value (%)	Calculated value (%)	Relative error (%)
298.15	0.0244	0.0251	2.73
303.15	0.0283	0.0276	−2.27
313.15	0.0327	0.0320	−1.95
323.15	0.0358	0.0356	−0.52
333.15	0.0377	0.0386	2.48
343.15	0.0405	0.0410	1.24
353.15	0.0437	0.0430	−1.73

$\pm 1.7\%$. The linear relationship between the experimental and calculated values is shown in Fig. 3, demonstrating that the model equation effectively describes the solubility behavior of lithium phosphate in water.

$$S\ (\%) = 0.0517 - 11.12\exp(-0.0202T)\ (R^2 = 0.9837) \quad (1)$$

$$\varepsilon = \left(m_{\mathrm{Li_3PO_4}}^{\mathrm{cal}} - m_{\mathrm{Li_3PO_4}}^{\mathrm{exp}}\right)\Big/ m_{\mathrm{Li_3PO_4}}^{\mathrm{exp}} \quad (2)$$

The solubility of Li_3PO_4 in Na_2CO_3 solutions was measured from 303.15 K to 353.15 K, with results displayed in Fig. 4 and Table 4. The relative deviations between experimental and calculated values are shown in Tables S2–S8,† with all errors within $\pm 2.7\%$. The linear relationship between the experimental and calculated values is shown in Fig. S1,† indicating a good fitting model for the solubility of Li_3PO_4 in Na_2CO_3 solutions.

It is noticeable that the addition of Na_2CO_3 significantly increased the solubility of Li_3PO_4, especially at higher dosages. However, when the mass fraction of Na_2CO_3 was more 15%, the solubility appeared to be near to the solubility limit values. This is because higher amounts of Na_2CO_3 would cause precipitation of Li_2CO_3, thus leading to a limit of solubility of the Li_3PO_4 in

solution. Thus, based on the salting-in effect of the Na_2CO_3 on the Li_3PO_4 solubility, it is necessary to remove carbonate ions from the lithium-bearing mother liquor to enable high yields of Li_3PO_4 during the crystallization process.

3.2 Supersolubility and MSZW of Li_3PO_4

In the experiments, the concentrations of LiCl solution, feeding rate, and stirring speed were set to $c_{\mathrm{Li+}} = 2$ g L^{-1}, 1 mL min^{-1}, and 250 rpm, respectively. As shown in Fig. 5, the supersolubility of Li_3PO_4 first increases and then decreases with the increase in Na_2CO_3 solution concentration, reaching a maximum value when the Na_2CO_3 concentration is 3%. This is mainly because the reactant concentration is the decisive factor driving the crystallization reaction. When the Na_2CO_3 concentration is low, the nuclei of Li_3PO_4 dissolve into the solution

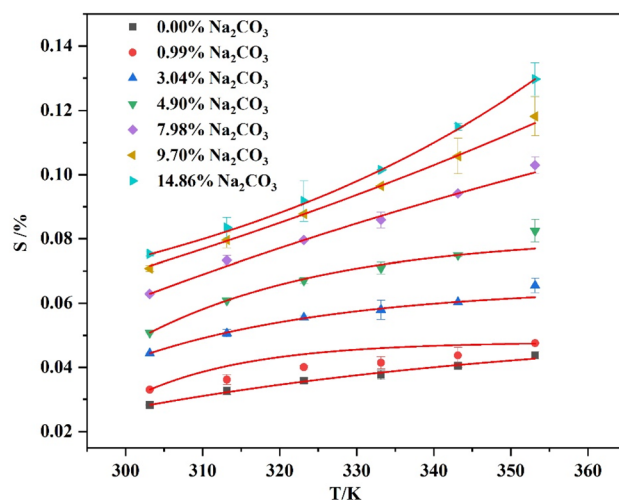Fig. 4 Solubility of Li_3PO_4 in sodium carbonate solutions as a function of temperature.

Table 4 Exponential solubility equations of Li_3PO_4 in sodium carbonates solutions at 303.15 K–353.15 K

Sodium carbonate concentration (%)	Exponential equation	R^2
0.99	$S = 0.0700 - 0.6271\exp(-0.0093T)$	0.9739
3.04	$S = 0.0798 - 5.3270\exp(-0.0166T)$	0.9736
4.90	$S = 0.1057 - 6.1802\exp(-0.0156T)$	0.9720
7.98	$S = 0.3899 - 0.6968\exp(-0.0025T)$	0.9899
9.70	$S = -0.0093 + 0.0051\exp(0.0091T)$	0.9806
14.86	$S = 0.0393 + 0.0001\exp(0.0182T)$	0.9993
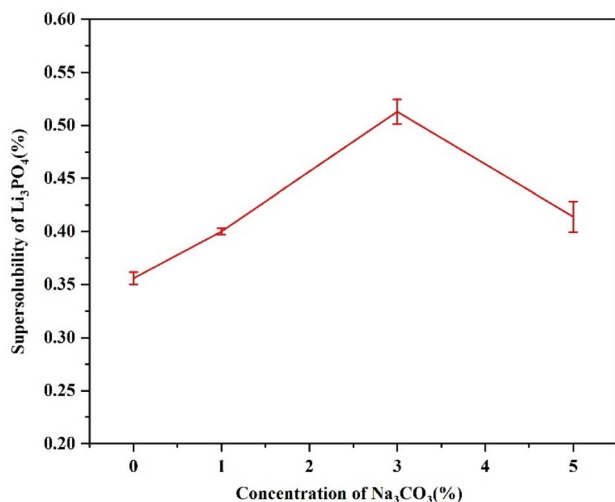
Fig. 5 The effect of sodium phosphate concentration on the supersolubility of lithium phosphate at 30 °C.

before being detected by the probe, delaying the crystallization reaction and leading to an increase in supersolubility. However, as the Na_2CO_3 concentration continues to increase, the higher concentration accelerates the crystallization reaction and nucleation rate, causing the nuclei to grow to a detectable size in a short time, which results in a decrease in supersolubility. Therefore, to ensure a wider metastable zone during the crystallization process, a Na_2CO_3 solution concentration of 3% was selected for the experiments.

Fig. 6 shows the solubility and supersolubility curves of Li_3PO_4 in a LiCl solution ($c_{Li+} = 2$ g L^{-1}). As can be seen from Fig. 6, compared to solubility, the supersolubility of Li_3PO_4 is more significantly affected by temperature, decreasing as the temperature increases. When the reaction temperature is 30 °C, the supersolubility is almost 15 times the solubility, whereas it became almost equal to the solubility at 80 °C, indicating that higher reaction temperatures can be used for lithium phosphate in practical production to obtain high yields. Supersolubility is the main driving force for crystallization and is influenced by various factors such as temperature, solute concentration, stirring conditions, feeding rate, and cooling rate. An increase in temperature promotes the movement of molecules or ions, thereby increasing the collision frequency
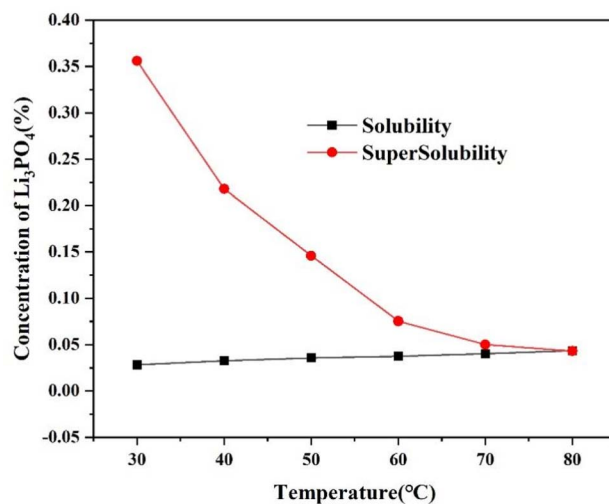
Fig. 6 The supersolubility and solubility of Li_3PO_4 in LiCl solution ($c_{Li+} = 2$ g L^{-1}).

and mass transfer rate between particles, accelerating nucleation, and leading to a reduction in supersolubility.

Fig. 7 and 8 showed the variation curves of the supersolubility and MSZW of Li_3PO_4 with the concentration of sodium carbonate. The supersolubility and MSZW of Li_3PO_4 first increased and then decreased with the addition of Na_2CO_3, which was not consistent with the effect on the solubility. According to Table 1, the equilibrium content of Li^+ and CO_3^{2-} ions in the mother liquor was 1.36 g L^{-1} and 17.33 g L^{-1} (about 2.62% in the form of Na_2CO_3), respectively. In our system, the lithium content used was 2 g L^{-1}, and the Na_2CO_3 concentration varied from 0.99%, 3.04% to 4.90%. The higher concentration of 4.90% may facilitate the Li_2CO_3 precipitation during the Li_3PO_4 crystallization, thus leading to a decrease in the supersolubility of Li_3PO_4, especially at lower temperatures. This
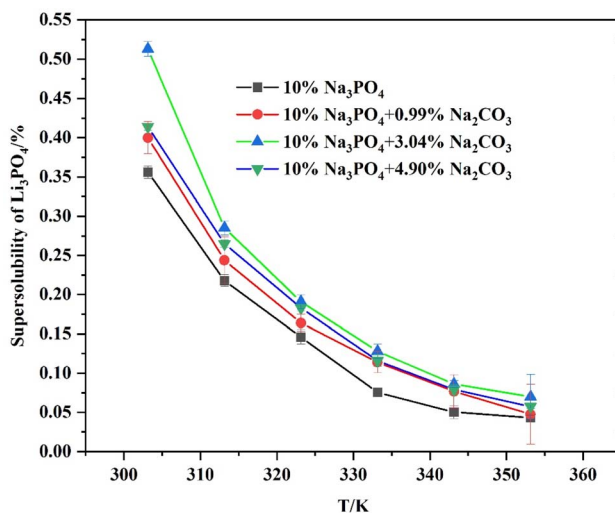
Fig. 7 The supersolubility curves of Li_3PO_4 in Na_2CO_3 systems with different concentrations.

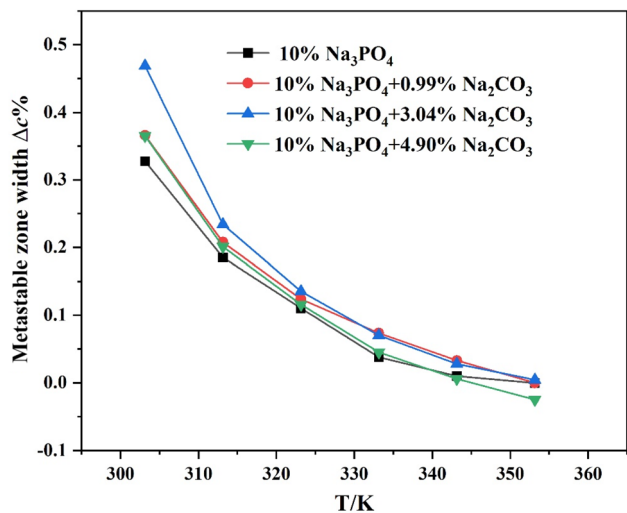Fig. 8 Metastable zone width of Li_3PO_4 in Na_2CO_3 electrolyte solution.

Fig. 9 Plot of the Gibbs free energy (ΔG_d) change *versus* temperature.

indicates that the role of CO_3^{2-} ion impurities in the crystallization process of Li_3PO_4 cannot be ignored. Therefore, to prepare the Li_3PO_4 product with high yield and purity, the removal of CO_3^{2-} ion impurities from the mother liquor is required.

3.3 The thermodynamic properties of Li_3PO_4 dissolution in Na_2CO_3 solutions

The Van't Hoff equation (eqn (3) reveals a linear relationship between the logarithm of the molar fraction of the solute and the reciprocal of absolute temperature. By assuming that the enthalpy (ΔH_d) and entropy (ΔS_d) of dissolution remain constant over the temperature range studied, the thermodynamic properties of Li_3PO_4 during dissolution in Na_2CO_3 solutions were calculated and shown in Table 5. The Gibbs free energy change (ΔG_d) during dissolution was also determined from eqn (4), as shown in Fig. 9.

$$\ln x = -\frac{\Delta H_d}{RT} + \frac{\Delta S_d}{R} \quad (3)$$

$$\Delta G_d = \Delta H_d - \Delta S_d T \quad (4)$$

The positive ΔG_d values indicate that the dissolution process is endothermic, and an increase in temperature favors the

dissolution of Li_3PO_4. As the Na_2CO_3 concentration increased, the ΔG_d values decreased, suggesting that higher Na_2CO_3 concentrations reduced the energy barrier for Li_3PO_4 dissolution, thereby enhancing its solubility by the salting-in effect.

3.4 Preparation of battery-grade Li_3PO_4

Based on the solubility and supersolubility of Li_3PO_4 in the Na_2CO_3 solutions, it is known that the effect of CO_3^{2-} ions on the crystallization process of Li_3PO_4 cannot be ignored. It is necessary to remove the CO_3^{2-} ion impurities from the mother liquor. Therefore, in this experiment, we first removed the CO_3^{2-} ions by adding hydrochloric acid until the mother liquor reached approximately pH 7.0; this was followed by the dropwise addition of an 8% sodium phosphate solution to prepare lithium phosphate. The yield and purity of lithium were investigated at 30 °C (sample LTS1) and 80 °C (sample LTS2). The lithium yield at 30 °C was only 15.23% after 24 hours, while it reached to 82.94% at 80 °C after 30 minutes. This is because Li_3PO_4 has a high supersolubility at low temperatures, which is not favorable for the crystal nucleation and growth of Li_3PO_4. The chemical analyses of the lithium phosphate product are shown in Table 6. Based on the content of PO_4^{3-}, the contents of Li_3PO_4 were calculated to be 84.05% and 80.898% for LTS1 and LTS2, respectively, with sodium ions as the primary impurity. Therefore, we purified the crude product obtained above using a hydrochloric acid recrystallization method (the process flow is shown in Fig. 10). The phase of the resulting

Table 5 The calculated ΔS_d and ΔH_d of Li_3PO_4 in Na_2CO_3 solutions

$\omega_{Na_2CO_3}$(%)	ΔS_d (J mol^{-1})	ΔH_d kJ (mol^{-1} K^{-1})
0	−55.44	−8.34
0.99	−61.49	−6.20
3.04	−57.88	−6.44
4.90	−51.50	−7.96
7.98	−48.22	−7.34
9.70	−45.47	−8.93
14.86	−42.46	−9.59

Table 6 Composition of Li_3PO_4

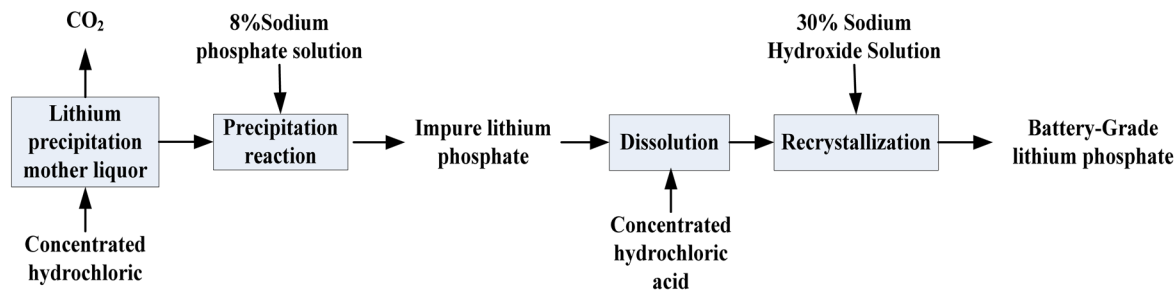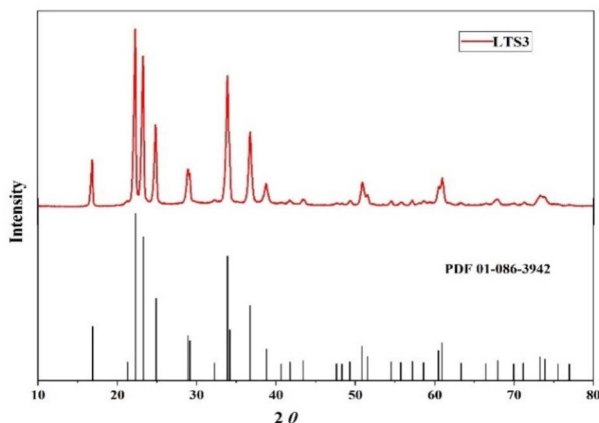| Sample	Li %	PO$_4$ %	Na %	K %	Mg %	Ca %
LTS1	16.04	68.93	2.48	0.053	0.052	0.059
LTS2	15.63	66.34	2.55	0.054	0.053	0.061
LTS3	18.15	79.96	0.078	0.035	0.012	0.066

Fig. 10 Process flow diagram for lithium phosphate preparation.

Fig. 11 XRD pattern of Li_3PO_4.

product (LTS3) is shown in Fig. 11. The peak positions in the XRD pattern of the sample were consistent with the standard card (PDF 01-086-3942), indicating that the prepared sample was pure-phase lithium phosphate. The chemical composition analysis of the sample is shown in Table 1, with the main component content calculated to be 99.80% based on phosphate content. This product can be used directly for the preparation of lithium iron phosphate cathode materials.

The structural variations information of the corresponding substances can be characterized by Raman spectroscopy. Fig. 12(a) shows the Raman spectra of lithium phosphate from 300 cm^{-1} to 1500 cm^{-1}. The clearly observed band at approximately 946.72 cm^{-1} in the lithium phosphate spectrum was attributed to the symmetrical stretching vibration of the P–O bond of PO_4^{3-}. For the asymmetric bending vibration (PO_4^{3-}), two bands are observed at 672.41 and 603.93 cm^{-1}. The band at

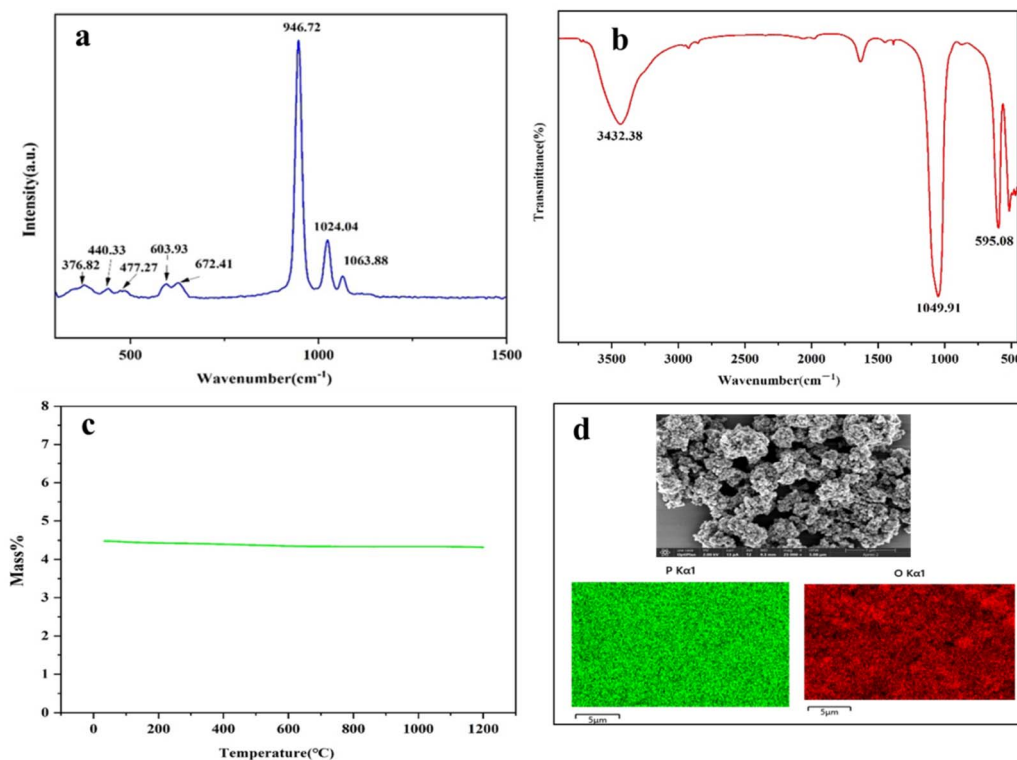Fig. 12 Raman (a), FTIR (b), TG (c) and SEM images (d) of lithium phosphate at 25 °C.

about 477.27 and 440.33 cm^{-1} was assigned to Li–O stretching vibrations.[38,39] The FTIR spectrum of lithium phosphate is shown in Fig. 12(b), which reveals characteristic absorption peaks at 1049.91 cm^{-1} and 541.8 cm^{-1} corresponding to stretching and asymmetrical stretching vibrations of PO_4^{3-}, respectively. The results of TG experiments with lithium phosphate, shown in Fig. 12(c), reveal that lithium phosphate remained undecomposed in the range of 30 °C to 1200 °C. From Raman, FTIR, TG and SEM analyses, it was concluded that the prepared lithium phosphate was pure phase. Fig. 12(d) shows an SEM image and EDS mapping spectrum of lithium phosphate. It can be clearly observed that the morphology of the lithium phosphate is non-uniform and blocky. The position and distribution of P and O elements can be clearly observed from Fig. 12(d). The content of P in lithium phosphate was lower than that of O, which was consistent with the composition of PO_4^{3-}. From Raman, FTIR, TG and SEM analyses, it was concluded that the prepared lithium phosphate was pure phase.

4. Conclusions

In this study, the solubility data of Li_3PO_4 in 0% to 14.86% Na_2CO_3 solutions was determined within the temperature range of 303.15 K to 353.15 K by using the dynamic dissolution equilibrium method. The effects of temperature and sodium carbonate concentration on the solubility of lithium phosphate were investigated, and the experimental data were correlated using an index equation. The results indicate that the solubility of lithium phosphate in pure water and sodium carbonate increases with rising temperature, but the change in solubility in pure water is relatively small. The solubility of lithium phosphate increases with the concentration of sodium carbonate due to two factors: the solubility of lithium carbonate being greater than that of Li_3PO_4 at the same temperature, and the salting-out effect of Na_2CO_3, which enhances the solubility of lithium phosphate. This suggests that high concentrations of Na_2CO_3 solution reduce the recovery rate of Li_3PO_4. The index equation can effectively describe the solubility properties of lithium phosphate. The supersolubility of lithium phosphate in different concentrations of sodium carbonate electrolyte solutions was measured using the turbidity method, and the MZW of Li_3PO_4 was calculated. The supersolubility of Li_3PO_4 is significantly influenced by temperature, decreasing as temperature increases, indicating that nucleation is slower at lower temperatures. The supersolubility of Li_3PO_4 first increases and then decreases with the concentration of Na_2CO_3 solution, reaching a maximum when the concentration of Na_2CO_3 is 3%, due to the reactant concentration being the decisive factor driving the crystallization reaction. The MZW of Li_3PO_4 decreases with increasing temperature. The thermodynamic functions ΔS_d, ΔH_d, and ΔG_d for the dissolution process of lithium phosphate were calculated based on the Van't Hoff equation. The dissolution is a spontaneous endothermic process. As the concentration of sodium carbonate increases, ΔG_d gradually decreases, indicating that higher Na_2CO_3 concentrations reduce the energy barrier for Li_3PO_4 dissolution, thereby enhancing its solubility by the salting-in effect. Based on the solubility and supersolubility data of Li_3PO_4 in pure water and sodium carbonate solutions, a new process for preparing battery-grade lithium phosphate from salt lake mother liquor by first acidification and then lithium precipitation was developed. The purities of the prepared lithium phosphate reached 99.80%. Raman, FTIR, TG and SEM analyses of Li_3PO_4 suggest that the prepared lithium phosphate was pure phase. This study provides fundamental physical chemistry data and theoretical support for the efficient separation and extraction of salt lake mother liquor.

Data availability

Data are present within the article.

Author contributions

Huaiyou Wang: methodology, investigation, formal analysis, and writing – original draft; Jia Zhang: investigation, formal analysis, and writing – review & editing; Xu Liu: software and measurement; Haiwen Ge: formal analysis and conceptualization; Zhibo Luo: measurement and supervision; Min Wang: funding acquisition, resources, and supervision. All the authors have read and agreed to the published version of the manuscript.

Conflicts of interest

There are no conflicts to declare.

Acknowledgements

References

1 Y. E. Milian, N. Jamett, C. Cruz, S. Herrera-León and J. Chacana-Olivares, A comprehensive review of emerging technologies for recycling spent lithium-ion batteries, *Sci. Total Environ.*, 2024, **910**, 168543, DOI: **10.1016/j.scitotenv.2023.168543**.

2 B. Swain, Recovery and recycling of lithium: A review, *Sep. Purif. Technol.*, 2017, **172**, 388–403, DOI: **10.1016/j.seppur.2016.08.031**.

3 A. Razmjou, M. Asadnia, E. Hosseini, A. Habibnejad Korayem and V. Chen, Design principles of ion selective nanostructured membranes for the extraction of lithium ions, *Nat. Commun.*, 2019, **10**, 5793, DOI: **10.1038/s41467-019-13648-7**.

4 J. Shin, J. M. Jeong, J. B. Lee, H. J. Cho, Y. H. Kim and T. Ryu, Preparation of lithium carbonate from waste lithium solution through precipitation and wet conversion methods, *Hydrometallurgy*, 2022, **210**, 105863, DOI: **10.1016/j.hydromet.2022.105863**.

5 J. Xiao, B. Niu and Z. Xu, Highly efficient selective recovery of lithium from spent lithium-ion batteries by thermal

reduction with cheap ammonia reagent, *J. Hazard. Mater.*, 2021, **418**, 126319, DOI: 10.1016/j.jhazmat.2021.126319.

6 S. A. Jose, J. L. Stoll, T. Smith, C. Jackson, T. Dieleman, E. Leath, N. Eastwood and P. L. Menezes, Critical Review of Lithium Recovery Methods: Advancements, Challenges, and Future Directions, *Processes*, 2024, **12**, 2203, DOI: 10.3390/pr12102203.

7 J. H. Han, Z. Nie, Z. H. Fang, Q. Wu, Q. Cao, Y. S. Wang, L. Z. Bu and J. J. Yu, Analysis of existing circumstance of supply and demand on China's lithiumresources, *Inorg. Chem.:Indian J.*, 2021, **53**, 61–66, DOI: 10.19964/j.issn.1006-4990.2021-0002.

8 T. Ding, M. P. Zheng, X. F. Zhang, Q. Wu and X. Y. Zhang, Development of lithium extraction technology and industrialization inbrines of salt lake, *Sci. Technol. Rev.*, 2020, **38**, 16–23.

9 C. Shi, H. Li, B. Liu, Y. Qin and G. Song, Solvent extraction of lithium from aqueous solution using an ammonium ionic liquid, *J. Mol. Liq.*, 2020, **304**, 112756, DOI: 10.1016/j.molliq.2020.112756.

10 T. Kanagasundaram, O. Murphy, M. N. Haji and J. J. Wilson, The recovery and separation of lithium by using solvent extraction methods, *Coord. Chem. Rev.*, 2024, **509**, 215727, DOI: 10.1016/j.ccr.2024.215727.

11 N. Kim, X. Su and C. Kim, Electrochemical lithium recovery system through the simultaneous lithium enrichment *via* sustainable redox reaction, *Chem. Eng. J.*, 2021, **420**, 127715, DOI: 10.1016/j.cej.2020.127715.

12 K. Zhao, J. Li, J. Yuan, X. Yu, Y. Guo, Z. Jiang, M. Li, J. Duo and T. Deng, A novel Co-doped H_2TiO_3 spinning composite for efficient lithium recovery from alkaline lithium precipitation mother liquor, *Chem. Eng. J.*, 2024, **482**, 148989, DOI: 10.1016/j.cej.2024.148989.

13 L. Zhang, H. P. Yang, L. Liu and G. F. Ding, Global Technology Trends of Lithium Extraction, *Conservation and Utilization of Mineral Resources*, 2020, **40**, 24–31, DOI: 10.13779/j.cnki.issn1001-0076.2020.05.004.

14 United States Pat.. US9988280, 2018.

15 X. Li, Y. Mo, W. Qing, S. Shao, C. Y. Tang and J. Li, Membrane-based technologies for lithium recovery from water lithium resources: A review, *J. Membr. Sci.*, 2019, **591**, 117317, DOI: 10.1016/j.memsci.2019.117317.

16 Y. Li, M. Wang, Y. J. Zhao, H. Y. Wang, H. J. Yang and Z. H. Zhu, Study on separation of magnesium and lithium from salt lake brine withhigh magnesium-to-lithium mass ratio by nanofiltration membrane, *CIESC journal*, 2021, **72**, 3130–3139, DOI: 10.11949/0438-1157.20201594.

17 H. Wen, Z. Liu, J. Xu and J. P. Chen, Nanofiltration membrane for enhancement in lithium recovery from salt-lake brine: A review, *Desalination*, 2024, **591**, 117967, DOI: 10.1016/j.desal.2024.117967.

18 Z. J. Cao, M. Gao, Z. Y. Ning and W. Wang, Lithium Resources and Lithium Extraction Technology in Qinghai Salt Lake, *Chem. Eng. Des. Commun.*, 2019, **45**, 190+207.

19 M. X. Li, *Master, Study on Lithium and Boron Extraction Process from Brine of Longmucuo Salt Lake in Tibet*, Jiangxi University Of Science And Technology, 2012.

20 J. Z. Qin, C. X. Li, X. L. Zhang and M. X. Xu, Difficulties and Prospects of the Production of Battery Grade LithiumCarbonate from Lithium Resources in Salt Lake, *J. Salt Sci. Chem. Ind.*, 2022, **51**, 15–18, DOI: 10.16570/j.cnki.issn1673-6850.2022.11.007.

21 N. Linneen, R. Bhave and D. Woerner, Purification of industrial grade lithium chloride for the recovery of high purity battery grade lithium carbonate, *Sep. Purif. Technol.*, 2019, **214**, 168–173, DOI: 10.1016/j.seppur.2018.05.020.

22 S. Xu, J. Song, Q. Bi, Q. Chen, W.-M. Zhang, Z. Qian, L. Zhang, S. Xu, N. Tang and T. He, Extraction of lithium from Chinese salt-lake brines by membranes: Design and practice, *J. Membr. Sci.*, 2021, **635**, 119441, DOI: 10.1016/j.memsci.2021.119441.

23 L. J. Li, C. L. Liu, X. F. Song and J. G. Yu, Optimization of Crystallization Process for Preparation of Lithium Phosphate in Alkaline SolutionSystem, *J. East China Univ. Sci. Technol.*, 2020, **46**, 598–607, DOI: 10.14135/j.cnki.1006-3080.20190430003.

24 C. Zhang, L. Wang, X. Ji and G. Li, Characterization of All Solid State Batteries with LiPON Thin Films Obtained with Different Substrates and RF Sputtering Times, *Mater. Trans.*, 2018, **59**, 1156–1160, DOI: 10.2320/matertrans.M2017419.

25 L. li, *Doctor, Study of Solid Electrolyte LiPON and All Solid-State Thin-Film Lithiumion Batteries' Fabrications and Characteristics*, Lanzhou University, 2018.

26 D. Y. Wang, *Master, Preparation of Li_3PO_4, Au/Li_3PO_4 and Isomerization Mechanism of Propylene Oxide Catalyzed by Li_3PO_4*, Nanjing University of Science and Technology, 2018.

27 Y. N. Wang and W. H. Ma, *Presented in Part at theSteam Treatment on Hollow Lithium Phosphate:enhancing Carbondeposition Resistance and Improving Their Catalytic Performances Ofpropylene Oxide Rearrangement*, Dalian, Liaoning, China, 2016.

28 W. Zhang, L. Chen, Z. Yang and J. Peng, An optical humidity sensor based on Li_3PO_4 hollow nanospheres, *Sens. Actuators, B*, 2011, **155**, 226–231, DOI: 10.1016/j.snb.2010.11.052.

29 A. Gassmann, C. Melzer and H. von Seggern, The Li3PO4/Al electrode: An alternative, efficient cathode for organic light-emitting diodes, *Synth. Met.*, 2012, **161**, 2575–2579, DOI: 10.1016/j.synthmet.2011.08.009.

30 C. Xiao and L. Zeng, Thermodynamic study on recovery of lithium using phosphate precipitation method, *Hydrometallurgy*, 2018, **178**, 283–286, DOI: 10.1016/j.hydromet.2018.05.001.

31 C. Zhao, Y. Zhang, H. Cao, X. Zheng, T. Van Gerven, Y. Hu and Z. Sun, Dataset of lithium phosphate recovery from a low concentrated lithium-containing solution, *Data Brief*, 2019, 25, 104044, DOI: 10.1016/j.dib.2019.104044.

32 D. F. Liu, J. C. Xiong, W. H. Xu, L. H. He, X. H. Liu and Z. W. Zhao, Lithium selective extraction from lithium-enriched solution by phosphate precipitation, *Chin. J. of Nonferrous Met.*, 2021, **31**, 2541–2550.

33 J. Z. Sun, Preparation of monodisperse micron lithium phosphate, *Ind. Miner. Process.*, 2008, 4–5, DOI: 10.16283/

j.cnki.hgkwyjg.2008.08.008, DOI: 10.16283/j.cnki.hgkwyjg.2008.08.008.

34 J. Zhu, X. P. Li, X. H. Liu, Y. Sun and J. Yu, Experimental Study on Purification of Crude Lithium Phosphate fromSalt Lake, *Min. Metall. Eng.*, 2023, **43**, 101–105, DOI: 10.3969/j.issn.0253-6099.2023.03.023.

35 RLD, *Handbook of Chemistry and Physics [M]*, 84th edn, CRC Pres, Boca Raton, 2004.

36 S. Wu, M. L. Zhang, C. Zan and H. Zhou, Process of Deep Recovery of Lithium from the Mother Liquor of Lithium Carbonate by Phosphate Precipitation, *J. Tianjin Univ. Sci. Technol.*, 2023, **38**(2), 35–41, DOI: 10.13364/j.issn.1672-6510.20220181.

37 BWDDEWHPV, *The NBS Tables of Chemical Thermodynamic Properties :selected Values for Inorganic and C1 and C2 Organic Sub-stances in SI Units [M]*, American Institute of Physics for the National Bureau of Standards, New York, 1982.

38 L. Popović, B. Manoun, D. de Waal, M. K. Nieuwoudt and J. D. Comins, Raman spectroscopic study of phase transitions in Li_3PO_4, *J. Raman Spectrosc.*, 2003, **34**, 77–83, DOI: 10.1002/jrs.954.

39 R. W. Berg, A. V. Nikiforov and N. J. Bjerrum, Vapor pressure and specific electrical conductivity in the H_2O–LiH_2PO_4–$LiPO_3$ system—a novel electrolyte for water electrolysis at elevated temperature, *Ionics*, 2021, **27**, 703–719, DOI: 10.1007/s11581-020-03867-0.